Tolerance and detoxification mechanisms to cadmium stress by hyperaccumulator *Erigeron annuus* include molecule synthesis in root exudate

Hong Zhang [a,b], Kate Heal [c], Xiangdong Zhu [d], Mulualem Tigabu [e], Yanan Xue [a,b], Chuifan Zhou [a,b,*]

[a] *College of Forestry, Fujian Agriculture and Forestry University, Fuzhou 350002, China*
[b] *National Positioning Observation and Research Station of Red Soil Hill Ecosystem in Changting, Fuzhou 350002, Fujian, China*
[c] *School of GeoSciences, The University of Edinburgh, Crew Building, Alexander Crum Brown Road, Edinburgh EH9 3FF, UK*
[d] *Shanghai Key Laboratory of Atmospheric Particle Pollution and Prevention (LAP3), Department of Environmental Science and Engineering, Fudan University, Shanghai 200433, China*
[e] *Swedish University of Agricultural Sciences, Faculty of Forest Science, Southern Swedish Forest Research Centre, PO Box 49, SE-230 53 Alnarp, Sweden*

ARTICLE INFO

ABSTRACT

Cadmium (Cd) is one of the most toxic environmental pollutants affecting the growth and reproduction of various plants. Analysis of the biological adaptation and tolerance mechanisms of the hyperaccumulator *Erigeron annuus* to Cd stress may help identify new plant species for phytoremediation and in optimizing the process. This study is to the first to analyze the molecular composition and diversity of dissolved organic matter (DOM) secreted by roots using FT-ICR MS, and multiple physiological and biochemical indexes of *E. annuus* seedlings grown in solutions containing 0–200 Cd μmol L^{-1}. The results showed that *E. annuus* had strong photosynthetic adaptation and protection ability under Cd stress. Cd was immobilized or compartmentalized by cell walls and vacuoles in the plant, thus alleviating Cd stress. Activation of anti-oxidation defense mechanisms also played an important role in alleviating or eliminating Cd toxicity in *E. annuus*. High Cd stress promoted production of a higher proportion of new molecules in DOM secreted by *E. annuus* roots compared to low Cd stress. DOM secreted by roots contributed to plant resistance to Cd-induced stress via producing more carbohydrates, aromatic structures and tannins. Results indicate the mechanisms underpinning the potential use of *E. annuus* as a phytoremediator in environments with moderate Cd pollution.

1. Introduction

Contamination of global soils by cadmium (Cd) has become increasingly widespread. Each year, about 3×10^4 t Cd enters the biosphere mainly from industrial and agricultural production activities (Annu et al., 2016; Sun et al., 2009; Xie et al., 2017). Cd is highly mobile, and may pose a potential hazard to plants, animals and human health through accumulation in the food chain (Han et al., 2018). Therefore, finding effective methods to remediate Cd-contaminated soil and reduce Cd damage to the environment is an ecological priority.

Much attention has been focused on the development and application of phytoremediation for the remediation and treatment of soil contaminated with potentially toxic elements (PTEs) as it is a low-cost and in-situ process (Zhu et al., 2019). Hyperaccumulator plants are the basis of phytoremediation, but, to date, the majority of the few plant species identified capable of Cd accumulation are slow growing, highly localized geographically and do not produce high biomass (Sun et al., 2009). Accordingly, identification of new Cd-hyperaccumulators with more favorable characteristics is required to advance phytoremediation of Cd-contaminated soils. *Erigeron annuus*, an invasive plant originating from North America, has been identified as a Cd-hyperaccumulator at lead-zinc mining areas in China (Wang et al., 2010). *E. annuus* produces high biomass and has a strong tillering ability without showing obvious toxic symptoms when grown at high Cd concentrations (100 μmol L^{-1}) (Wang et al., 2010). However, the mechanisms of tolerance and detoxification of Cd by *E. annuus* are largely unknown, which greatly restricts

---

its application for phytoremediation of Cd-contaminated land.

In order to alleviate the damage caused by Cd stress, plants have evolved a number of tolerance and detoxification mechanisms, including production of anti-oxidants, cell wall precipitation and vacuolar compartmentalization, Cd chelation and secretion of root organic matter (some secretions can combine with Cd^{2+}, reducing the absorption of Cd by plants) (Pinto et al., 2008; Fu et al., 2011; Zhou et al., 2015). The composition and quantity of plant root exudates can change considerably under PTE stress. Root exudates usually comprise low and high molecular weight compounds, yet previous studies of plant tolerance and detoxification mechanisms have mainly focused on the former (Bais et al., 2006; Pinto et al., 2008; Zhao and Wu, 2018). As a result, the overall molecular composition of dissolved organic matter (DOM) secreted by roots is unknown. The low concentration, high polarity and extreme complexity of this material make it difficult to obtain molecular level information using standard techniques.

Recently, Fourier transform ion cyclotron resonance mass spectrometry (FT-ICR MS) at high magnetic fields (> 9 T) coupled with negative electrospray ionization (ESI) has proven to be advantageous in determining DOM composition in environmental samples (Yuan et al., 2017), such as marine waters, fresh waters, Arctic soils and paddy soils (Seidel et al., 2015; Wagner et al., 2015; Chen et al., 2018; Li et al., 2018). Due to its ultrahigh resolution and high mass accuracy, the exact molecular formulae of compounds in DOM can be determined, including those containing heteroatoms, e.g., nitrogen and sulfur (Hao et al., 2018). Thus, ESI FT-ICR MS provides the capability to elucidate the composition of DOM released from the roots of PTE-stressed plants and hence potential mechanisms of root tolerance to PTEs.

We used *E. annuus* as a model Cd hyperaccumulator to investigate its tolerance and detoxification mechanisms to Cd stress through physiological and biochemical analysis. Specifically, the chemical composition of DOM secreted by roots was determined by ESI FT-ICR MS to investigate in detail the tolerance mechanisms under Cd stress. We examined the effectiveness of changes in molecular composition and diversity of DOM secreted by roots, coupled with anti-oxidation defense mechanisms and compartmentalization of absorbed Cd, as mechanisms of tolerance and detoxification of Cd by *E. annuus*. To the best of our knowledge, this is the first study to comprehensively characterize the DOM secreted by roots, as well as to analyze changes in the molecular composition and diversity of DOM secreted by roots under different Cd concentrations. The results will help increase understanding of the tolerance and detoxification mechanisms of plants to PTEs and provide new directions for phytoremediation of PTE-contaminated soil.

2. Materials and methods

2.1. Plant culture and harvest

Whole *E. annuus* plants with an aboveground height of ~10 cm were collected on 16 March 2018 from uncultivated land on the campus of Fujian Agricultural and Forestry University, Fuzhou, Fujian Province, China. Properties of the campus soil are shown in Supporting Information S1. Plants were cleaned with tap water and pre-cultured for 3 days in ultrapure water (18.25 MΩ cm^{-1}). Afterwards, plants of similar size were transplanted and cultured in individual round plastic pots (15 cm diameter, 10 cm height) for 2 weeks with Hoagland nutrient solution, changed every 3 days. Plants with uniform size and intact roots were then selected and transferred into round plastic pots for exposure culture, where Cd (as $CdCl_2$ solution) was added to Hoagland nutrient solution at Cd concentrations of 0, 25, 50, 100, 200 µmol L^{-1} (corresponding to $CdCl_2$ concentrations of 0, 29.2, 58.9, 115, 209 µmol L^{-1}). Culture conditions as detailed in Supporting Information S2. Each treatment was replicated 4 times, with 3 *E. annuus* plants per pot (i.e. 12 plants in each treatment).

The whole plants were harvested for analysis after 15 days of Cd exposure. The fresh weight of the whole plant and maximum lengths of the aboveground (tallest stem) and underground (longest root) parts were recorded. Next, the 12 plants in each treatment were divided into 3 sub-samples to provide 3 replicate samples of each treatment. Plants were washed with tap water and roots were soaked in 20 mmol L^{-1} Na_2-EDTA for 15 min to remove Cd adsorbed on the root surface (Du et al., 2011), then rinsed thoroughly in ultrapure water, blotted dry with tissues to remove surface moisture, and divided into three parts: roots, stems and leaves. Sub-samples of roots, stems and leaves were frozen in liquid N_2 and stored at $-80\ °C$ for biochemical analyses. The remaining materials were oven-dried at 105 ºC for 30 min and then at 80 °C to constant mass.

2.2. Measurement of chlorophyll fluorescence parameters

The day before plant harvesting, chlorophyll fluorescence parameters of *E. annuus* leaves under different Cd concentrations were determined as detailed in Supporting Information S3.

2.3. Determination of bulk and subcellular fractions of Cd

Sub-samples of dried roots, stems and leaves were weighed (0.2 g), ground to a fine powder, and digested with acid solution containing 8 mL HNO_3 and 2 mL $HClO_4$ (4:1, v/v) at 200 °C until the solution became clear. Then, the digested samples were made up to 25 mL with 1% HNO_3 solution and filtered through a 0.45 µm filtration membrane. The concentrations of Cd in the digests were determined by ICP-OES (Optima 8000, PerkinElmer, USA). The subcellular fractions of Cd in roots, stems and leaves of *E. annuus* (frozen in liquid N_2 as described in Section 2.1) were extracted for the 0, 25 and 200 µmol L^{-1} Cd treatments, following the method of Zhou et al. (2017) using differential centrifugation with some modification. Cadmium concentrations were determined in digests of these subcellular fractions using the same procedures as described above. Details of methods and quality control are provided in Supporting Information S4.

2.4. Assessment of plant ultrastructure by transmission electron microscopy and energy dispersive X-ray analysis

Samples of fresh root tips (1–3 cm in length) and leaf Sections (1–3 cm) from the middle section of the third leaf from the stem top of *E. annuus* exposed to 0, 25 and 200 µmol L^{-1} Cd for 15 days were selected for TEM-EDS analysis (details in Supporting Information S5).

2.5. Analysis of lipid peroxidation, antioxidant enzyme activities and root plasma membrane integrity

Fresh leaf and root samples (0.2 g fresh weight) were homogenized and centrifuged to obtain supernatant, used to determine lipid peroxidation and superoxide dismutase (SOD), catalase (CAT), peroxidase (POD) activities. Lipid peroxidation was determined according to Yamamoto et al. (2001) and Islam et al. (2008) with minor modification, using a thiobarbituric acid (TBA) assay to measure the concentration of malondialdehyde (MDA), an end product of lipid peroxidation. The activities of SOD, POD and CAT were determined following the method of Gupta et al. (2010), Zhou et al. (2017), and Islam et al. (2008), respectively. During harvesting, roots (2 cm) of plants from each treatment were stained with Evans blue solution [0.025% (w/v) Evans blue in 100 µmol L^{-1} $CaCl_2$ (pH 5.6)] for 30 min for histochemical detection of loss in plasma membrane integrity in root apices of *E. annuus* (Yamamoto et al., 2001). Details of the methods are provided in Supporting Information S6.

2.6. Assay of non-enzymatic physiological features

Concentrations of proline, non-protein thiols (NPT) and reduced glutathione (GSH) were measured in fresh leaf and root samples using

the methods of Bates et al. (1973), Zhou et al. (2015) and Hissin and Hilf (1976) with some modifications (details in Supporting Information S7). Phytochelatin (PC) concentration was estimated by subtracting the GSH concentration from the NPT concentration.

2.7. Collection of root exudates and FT-ICR MS analysis

After harvesting the plants, the nutrient solution in the pots for the 0, 25, and 200 µmol L^{-1} Cd treatments was transferred separately to a 500 mL glass beaker, filtered through a 0.45 µm membrane, and the filtrate stored at 4 °C for 1 day before FT-ICR MS analysis. In preparation for FT-ICR MS analysis, 200 mL filtered sample was acidified with HCl to pH 2, before passing through an activated solid phase extraction column (Agilent Bond Elut PPL cartridges), previously rinsed with pure methanol and acidified Milli-Q water (pH 2). After extraction, the cartridges were completely dried with ultrapure N_2 gas, and DOM was immediately eluted with LC-MS grade methanol (10 mL). The DOM samples were diluted with methanol to produce a 0.2 mg mL^{-1} solution (Yuan et al., 2017). All extracted DOM samples were analyzed using a Bruker Apex ultra FT-ICR MS equipped with a 9.4 T superconducting magnet. The prepared solutions were directly injected into the electrospray ionization (ESI) source at a rate of 180 µL h^{-1} using a syringe pump. The ESI charge can preferentially ionize polar heteroatom compounds (e.g. nitrogen and sulfur) in the presence of hydrocarbons. Here, negative ESI mode was used as it favors detection of molecules with acidic functional groups that deprotonate, such as carboxylic acids, and thus is the mode commonly used in studies of natural organic matter (e.g. Yuan et al., 2017; Li et al., 2018). Conditions for negative-ion formation typically consisted of 4.0 kV spray shield voltage, 4.5 kV capillary voltage and − 320 V capillary column end voltage. The mass range was set at m/z 100–800. For improving the signal-to-noise ratio and dynamic range, the data size was set to 4 M words, and 128 scan FT-ICR data sets were accumulated (Hao et al., 2018). Detailed information on mass calibration, data acquisition and processing of FT-ICR MS have been reported previously (Lv et al., 2016; Yuan et al., 2017).

2.8. Statistical analysis

All data are reported as mean values ± standard deviation (SD) of three replicate samples for each treatment as explained earlier, apart from the FT-ICR MS analysis results for the root exudate DOM (n = 1). With the exception of the root exudate DOM data, significant differences between data from different Cd treatments were analyzed by one-way Analysis of Variance (ANOVA), with multiple comparisons among the treatment mean values conducted using Least Significant Difference (LSD) tests. All analyses were conducted with SPSS version 19.0 for Windows, and the significance level used was $p < 0.05$.

3. Results and discussion

3.1. Plant growth and leaf chlorophyll fluorescence characteristics

Plant growth of *E. annuus* was normal at Cd concentrations ≤ 50 µmol L^{-1}. However, visual root browning and leaf wilting were observed at Cd concentrations ≥ 100 µmol L^{-1} (Table S2). Maximum plant height and fresh weight of *E. annuus* occurred in the 25 µmol L^{-1} Cd treatment, and then decreased with increasing Cd concentrations, while maximum root length increased with increasing Cd exposure (Table S2). These results indicated that exposure to Cd could enhance the growth of *E. annuus* at low concentration (≤ 25 µmol L^{-1}), but slightly inhibit growth at high Cd concentration (≥ 100 µmol L^{-1}).

Chlorophyll fluorescence parameters F_M and F_0 were highest at 0 and 25 µmol L^{-1} Cd, and then decreased significantly with increasing Cd concentration (Fig. 1a, b), indicating that the electron transmission of *E. annuus* leaves decreased at the lowest Cd exposure concentration, whilst the photo-protection mechanism was activated at Cd concentrations ≥ 50 µmol L^{-1} (Demmig et al., 1987; Ekmekçi et al., 2008). Usually, F_V/F_M is constant under non-stressed conditions and decreases under stressed conditions (Heraud and Beardall, 2000). In this study there was no significant difference ($p > 0.05$) in F_V/F_M between the control and Cd treatments (Fig. 1c), indicating no significant change in
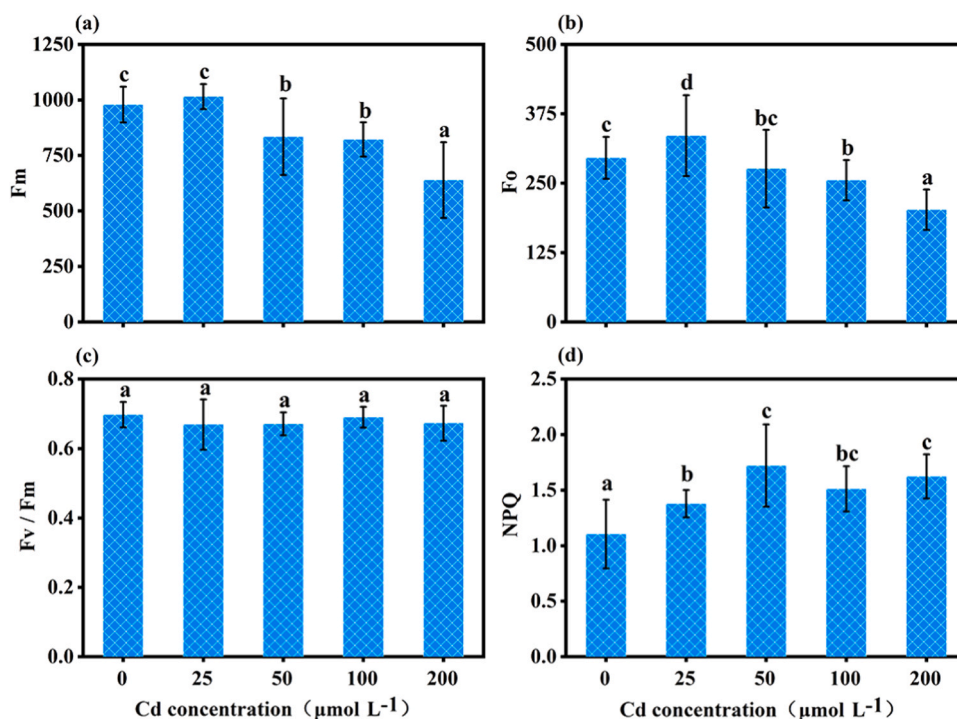
Fig. 1. Chlorophyll fluorescence parameters in leaves of *E. annuus* grown in solutions of different Cd concentrations for 15 days. (a) Maximum fluorescence (F_M). (b) Minimum fluorescence (F_0). (c) Maximum quantum yield of PSII (F_V/F_M). (d) Non-photochemical quenching coefficient (NPQ). The data represent the mean ± S.D. of three replicates. Different letters above the bars indicate significant differences among treatments at $p < 0.05$ level according to the LSD test.

conversion efficiency of light energy in *E. annuus* leaves exposed to Cd. These results differ from those of Ekmekçi et al. (2008), who reported that F_V/F_M decreased significantly in leaves of two maize cultivars due to Cd exposure. In our study, the non-photochemical quenching coefficient (NPQ) increased significantly ($p < 0.05$) compared to the control with increasing Cd concentration up to the 50 µmol L^{-1} Cd treatment and then stabilized at higher values in the 100 and 200 µmol L^{-1} Cd treatments (Fig. 1d). This indicates that the non-photochemical quenching of maximal chlorophyll fluorescence was increased initially by Cd stress, which allowed excessive heat energy within the photosystems to dissipate, protecting the photosynthetic structures from photo-oxidation damage caused by Cd stress (Yuan et al., 2014; Zhao et al., 2018), but that this response may only be activated up to a certain stress threshold. A similar pattern of NPQ response to increasing Cd stress was reported by Huang et al. (2017) for tall fescue grass, which has also shown potential for phytoremediation of soils contaminated with potentially toxic elements. NPQ values in tall fescue seedlings increased significantly compared to the control for the lowest Cd treatment (1 mg L^{-1} Cd ≈ 8.9 µmol L^{-1} Cd), then stabilized at the 44.5 and 444 µmol L^{-1} treatments, before increasing again in the highest Cd treatment (1334 µmol L^{-1} Cd). In contrast, NPQ values did not change significantly compared to the control treatment in seedlings of two maize cultivars watered with nutrient solution containing up to 300, 600 and 900 µmol L^{-1} Cd (Ekmekçi et al., 2008). This difference could be because the threshold for response to Cd stress was exceeded in all the relatively high Cd concentrations used in the latter experiment, or be due to physiological differences between different plants. Overall, the changes measured in chlorophyll fluorescence parameters indicated that *E. annuus* has strong photosynthetic adaptation and protection ability under Cd stress.

3.2. Cd accumulation and distribution in whole plant tissues and subcellular fractions

Cd concentration in the roots, stems, and leaves of *E. annuus* increased significantly with increasing Cd exposure (Table 1) as reported for other plants, e.g. *C. canadensis* (Zhou et al., 2015). When the Cd exposure concentration was ≤ 50 µmol L^{-1}, the Cd concentration in plant tissues was in the order: roots > leaves > stems, whilst at higher Cd exposure concentrations the stems contained higher Cd concentrations than the leaves. Greater Cd accumulation occurred in roots than in leaves and stems, which is attributed to mechanisms that prevent the transfer of PTEs from the plant root to the aboveground parts, such as interception in the root endodermis, particularly by the casparian strip (Zhou et al., 2017). Root Cd concentrations increased markedly between the 50 and 100 µmol L^{-1} Cd exposure concentrations, but then stabilized in the 200 µmol L^{-1} Cd treatment. Similar patterns between root Cd concentration and Cd exposure have been reported for different plants grown in Cd-contaminated soil (Sun et al., 2009; Zhou et al., 2015). We suggest that it could be caused by a combination of enhanced Cd uptake at higher exposure concentrations when plant defense mechanisms may be overwhelmed and stunting of plant growth due to

the increasingly toxic effects of Cd (as evident in the images of *E. annuus* in the current study in Table S2).

The subcellular distribution of Cd in *E. annuus* roots, stems and leaves, is shown in Fig. 2. Overall, the Cd content in the different subcellular fractions increased with increasing Cd concentration, particularly in the plants treated with 200 µmol L^{-1}. In roots and leaves of *E. annuus* Cd was contained predominantly in the cell wall, followed by soluble constituents, whilst the order was reversed in stems. As the outer tissue structure of plant cells, the cell wall of roots is the first barrier to protect cell protoplasts from PTEs. It is composed mainly of cellulose, hemicellulose, pectin and protein, providing a variety of negatively charged organic groups (Fu et al., 2011). These can effectively bind Cd ions and prevent them from entering into the cells, thus reducing the impact on plant cells. In this study, most of the accumulated Cd was stored in the cell walls of both leaves and roots of *E. annuus* (Fig. 2), suggesting that the cell wall plays a significant role in Cd tolerance of plants. In contrast, in *Phytolacca americana* L. the largest proportion of Cd (53.7–68.3%) was reported in the soluble subcellular fraction in roots and leaves (Fu et al., 2011). Similarly, we showed that Cd was primarily concentrated in the soluble constituents (including vacuoles and cytoplasm) in stems of *E. annuus*, indicating that Cd ions were transferred into vacuoles for storage. Vacuoles contain organic acids, alkaloids and
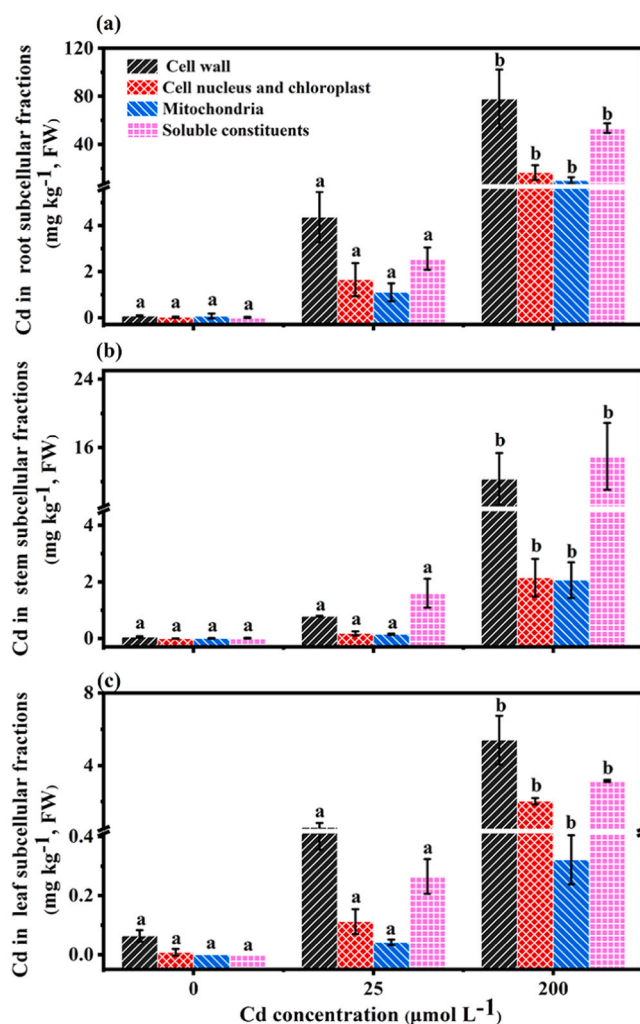
Fig. 2. Subcellular distribution of Cd (mg kg^{-1}, fresh weight) in (a) root, (b) stem and (c) leaf compartments of *E. annuus* exposed to 0, 25 and 200 µmol L^{-1} Cd for 15 days. The data represent the mean ± S.D. of independent leaves, one on each of three separate plants in each treatment. Different letters in the same fraction indicate significant differences among treatments at $p < 0.05$ level according to the LSD test. Note different y-axis scales.

Table 1
Concentrations of Cd (mg kg^{-1}) in the root, stem and leaf compartments of *Erigeron annuus* after exposure to different Cd concentrations for 15 d. Data in the same column followed by different letters indicate significant differences among treatments at $p < 0.05$ level according to the LSD test. Values are means ± standard deviation (n = 3).

Cd exposure concentrations (µmol L^{-1})	Cd concentration in plant tissue compartments (mg kg^{-1})		
	Root	Stem	Leaf
0	0.10 ± 0.26a	0.44 ± 0.21a	1.46 ± 0.63a
25	17.0 ± 4.34ab	3.03 ± 0.22a	6.12 ± 0.84a
50	33.3 ± 13.0b	20.2 ± 0.94ab	15.2 ± 4.37b
100	174 ± 7.09c	68.7 ± 38.5b	36.9 ± 3.34c
200	197 ± 3.90c	100 ± 46.5c	78.3 ± 3.97d

proteins, which can form chelate complexes with Cd ions and alleviate the toxic effects of Cd on plants, and therefore form a secondary barrier to protect plant cell protoplasts from PTEs (Verkleij et al., 1990).

3.3. Effect of Cd on plant ultrastructure

Ultrastructural observations on root meristematic cells of *E. annuus* grown in the control conditions without Cd showed that these cells had abundant cytoplasm and were filled with numerous organelles without any obvious damage (Fig. 3a, panel a and b). Cells possessed clear, smooth and continuous walls and membranes. Under the 25 and 200 μmol L^{-1} Cd treatments, the root meristematic cells exhibited ultrastructural changes compared to the control (Fig. 3a, panel c-f), such as increased vacuolation, swollen mitochondria, damaged membranes and loose cell wall structure, and the effects increased with increasing Cd concentrations. In addition, we observed black precipitates in intercellular spaces, on the inner and outer sides of cell walls and inside cell vacuoles (Fig. 3a, panel d and f). EDS analysis of these black precipitates revealed that they contained Cd, C, O and Cl (Fig. S1).

Transmission electron micrographs of the leaf mesophyll cells of *E. annuus* are shown in Fig. 3b. In the control, chloroplasts were ellipsoidal-shaped with intact chloroplast membranes and the thylakoid membranes of the stroma and grana exhibited a regular arrangement (Fig. 3b, panel a and b). There were few starch grains and osmophilic granules in the chloroplasts. In treatments with lower Cd concentrations, the chloroplast shape changed very slightly with clear and regular thylakoid membranes (Fig. 3b, panel c and d). Under the 200 μmol L^{-1} Cd treatment, abnormal-shaped chloroplasts with severe internal structural distortion were observed. Some had an irregular outline, and the thylakoid membranes were disordered or dissolved. Moreover, the intercellular space was enlarged (Fig. 3b, panel e and f) and the black precipitates in the cells and vacuoles contained Cd (Fig. S2).

These results indicated that Cd was deposited in cell walls, intercellular spaces and vacuoles of Cd-exposed *E. annuus*, resulting in damage to mitochondria, chloroplasts and membrane systems. In agreement with the results obtained from the analyses of subcellular fractions (Fig. 2), the ultrastructural analysis confirmed that the root cell wall and root and leaf vacuoles were the main reservoirs for Cd and played an important role in plant tolerance to Cd.

3.4. Effect of Cd on membrane integrity and the antioxidant defense system

Evan's blue staining analysis revealed that root tips were more strongly stained with increasing Cd concentration (Fig. S3), indicating a loss of plasma membrane integrity under Cd stress. Similarly, the malondialdehyde (MDA) concentration in leaves and roots was significantly higher compared with the control in the 200 μmol L^{-1} Cd treatment and also for the roots exposed to 100 μmol L^{-1} Cd (Fig. 4a), indicating damage to cell membranes and lipid peroxidation. MDA is a general indicator of the extent of lipid peroxidation initiated by oxidative stress (Monteiro et al., 2009), and is produced from the reaction between free radicals and polyunsaturated fatty acids in bio-membranes, which is involved in generating HO_2^-. HO_2^- is a much stronger oxidant than superoxide anion radicals and can induce the chain oxidation of polyunsaturated phospholipids, thus resulting in impairment of membrane function (Zhou et al., 2017). In the present study, MDA concentrations in *E. annuus* were much greater in roots than in leaves in all treatments (Fig. 4a), indicating that cell membrane damage and lipid peroxidation affected roots of *E. annuus* more than leaves.

Increased activity of antioxidant enzymes, such as SOD, CAT, and POD, is considered to play an important metabolic role in the cellular defense strategy against oxidative stress caused by PTE exposure (Van Assche and Clijsters, 1990). In this study, both SOD and CAT activities showed the same trends, with the maximum activity in roots occurring at 50 μmol L^{-1} Cd followed by a decrease with increasing Cd concentration, whilst in leaves the maximum occurred at 100 μmol L^{-1} Cd (Fig. 4b and c). In contrast, the activity of POD in roots initially increased before declining sharply with increasing Cd concentration, while POD activity in leaves increased up to the 50 μmol L^{-1} Cd treatment and then remained stable (Fig. 4d).

(a) Root　　　　**(b) Leaf**
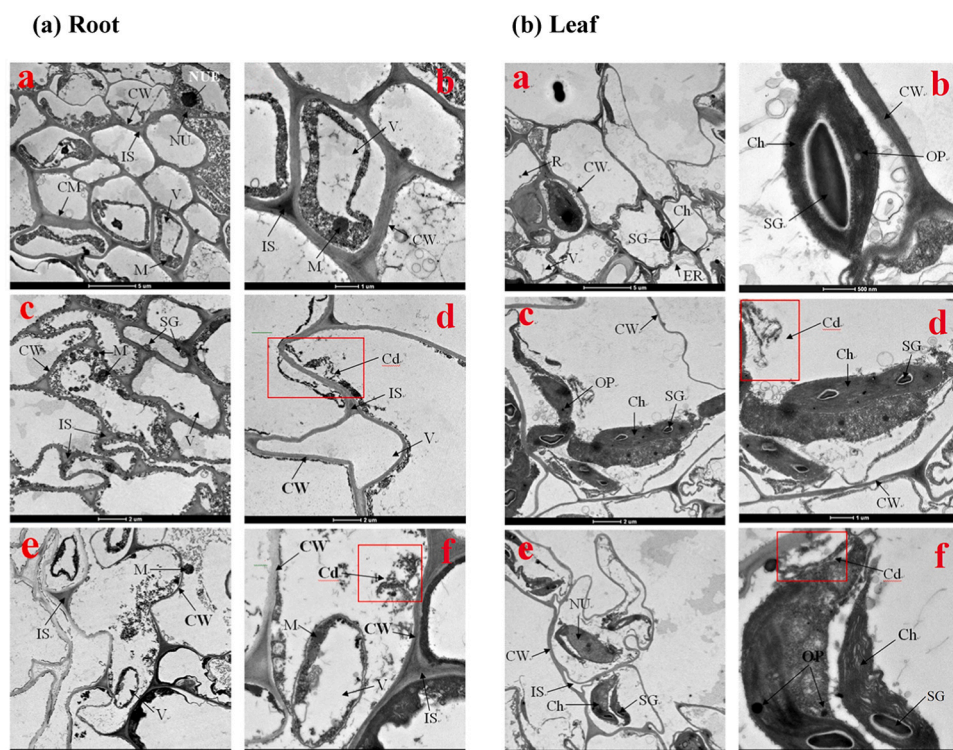
Fig. 3. Transmission electron micrographs of (a) root and (b) leaf meristematic cells from *E. annuus* exposed to (panel a and b) 0, (panel c and d) 25 and (panel e and f) 200 μmol L^{-1} Cd for 15 days, respectively. Labels: CW, cell wall; CM, cell membrane; NU, nucleus; NUE, nucleolus; V, vacuole; IS, intercellular space; SG, starch grain; M, mitochondria; CH, chloroplast; OP, osmiophilic particle; ER, endoplasmic reticulum; R, ribosome. Black precipitates in the boxes outlined in red in a (panel d and f) and b (panel d and f) were shown by EDS analysis to contain Cd. (For interpretation of the references to color in this figure legend, the reader is referred to the web version of this article.)
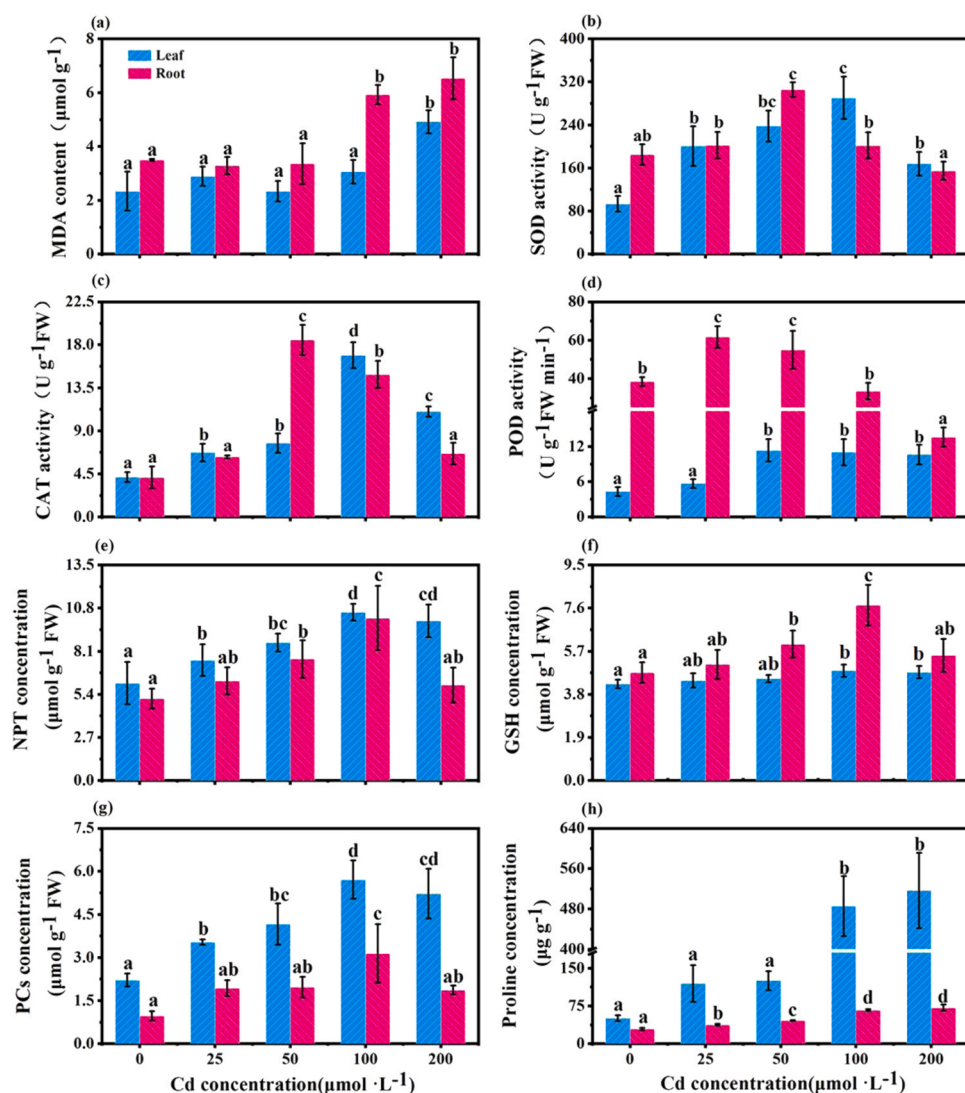
Fig. 4. (a) Malondialdehyde (MDA) concentration (for assessing lipid peroxidation), (b) superoxide dismutase (SOD), (c) catalase (CAT), (d) peroxidase (POD) activities, (e) non-protein thiols (NPT), (f) glutathione (GSH), (g) phytochelatins (PCs) and (h) proline concentrations in leaf and root compartments of *E. annuus* grown in solutions of different Cd concentrations for 15 d. The data represent the mean ± S.D. of three independent replicates. Different letters above the bars indicate significant differences among treatments at $p < 0.05$ level according to the LSD test for leaf/root compartments separately.

The increase in SOD activity at lower Cd concentrations (Fig. 4b) may be a result of the production of $O_2^{\bullet-}$, which stimulates SOD activity. However, SOD activity decreased significantly at higher Cd concentrations, which might be due to oxidative damage of antioxidant enzymes, thereby reducing their activities (Islam et al., 2008). The activities of SOD and CAT in leaves (Fig. 4b and c) exceeded those in roots at higher Cd concentrations, indicating that SOD and CAT may play a more important role in Cd detoxification in leaves of *E. annuus*. Conversely, the higher activity of POD in roots compared to leaves (Fig. 4d) implies that POD played a more important role in detoxification in *E. annuus* roots.

Non-enzymatic antioxidants are another strategy for plants to cope with PTE stress, and include non-protein thiols (NPT), glutathione (GSH), phytochelatins (PCs) and proline (Gill and Tuteja, 2010). With increasing Cd concentration, NPT, GSH, and PCs concentrations in roots and leaves of *E. annuus* first increased significantly compared to the control, to maximum values in the 100 µmol L⁻¹ Cd treatment, and then decreased (Fig. 4e-g). The exception to this pattern was GSH concentrations in leaves, which increased significantly only in the highest Cd treatments (Fig. 4f). The proline concentration in the roots increased significantly compared to the control with increasing Cd concentration and in all Cd treatments, while that in leaves was only significantly higher compared to the control in ≥ 100 µmol L⁻¹ Cd treatments (Fig. 4h).

GSH and PCs are important components of NPT, and increasing NPT induces synthesis of all or some of these constituents, which play an important role in PTE detoxification processes in plants (Gupta et al., 2010; Zhou et al., 2015). In previous studies, increased NPT concentrations have been associated with enhanced S assimilation due to the over-expression of genes responsible for this process and the active participation of NPT in the detoxification of Cd (Namdjoyan et al., 2012; Zhou et al., 2015). GSH is a direct precursor in PC synthesis, considered the most important intracellular defense against ROS-induced oxidative damage (Gill and Tuteja, 2010). We found significantly higher GSH concentrations in roots and leaves of *E. annuus* exposed to 50 and 100 µmol L⁻¹ Cd concentrations compared to the control (Fig. 4f), which may be attributed to enhanced GSH production to maintain increased PC synthesis in Cd stressed plants, as previously demonstrated by Rüegsegger et al. (1990). In the present study, PCs concentrations in roots and leaves were significantly higher than the control in all Cd treatments (apart from leaves at 200 µmol L⁻¹ Cd) (Fig. 4g), indicating that *E. annuus* increases PC synthesis to reduce Cd toxicity.

Our results suggest that different tissues of *E. annuus* resist Cd stress by inducing the synthesis of different non-enzymatic antioxidants. It had been reported that PC was relatively more important in roots, while GSH appeared to be more important in leaves (Estrella-Gómez et al., 2012). In contrast, we found that GSH played a more significant role in root detoxification, while PCs concentrations were greater in leaves

compared to roots of *E. annuus*. As well as being an osmolyte, proline is now considered a non-enzymatic antioxidant that microbes and plants require to mitigate the adverse effects of ROS (Gill and Tuteja, 2010). In the present study, we found that Cd stress leads to a rapid accumulation of proline in *E. annuus*, particularly in leaves (Fig. 4h). This indicates that plants can reduce unfavorable effects of Cd stress by accumulating proline (Yang et al., 2009), but the possible metabolic pathways leading to Cd-induced proline accumulation are still to be identified.

3.5. Detoxification mechanisms by DOM from root secretion

To investigate the relationship between DOM secreted by roots of *E. annuus* and Cd detoxification, FT-ICR MS was used to identify the chemical constituents of this DOM. The majority of molecules in the liquid phase had masses of 150–600 m/z. Peak relative abundance of low molecular weight compounds in the range 300–350 m/z was highest for the 25 μmol L^{-1} Cd treatment and suppressed in plants exposed to the 200 μmol L^{-1} Cd treatment (Fig. S4a). The carbon number of root exudate DOM was shifted to lower values for the plants exposed to Cd (Fig. S4b), indicating that Cd stress may promote secretion by roots of DOM constituents with lower carbon numbers (Zhu et al., 2019). The opposite pattern was observed for the relative abundance of Ox compounds. Root exudate DOM from the control contained mainly O_3 compounds, while that from plants exposed to 25 and 200 μmol L^{-1} Cd contained mainly O_5 and O_6 compounds and O_7 and O_8 compounds, respectively (Fig. S4c), indicating that Cd stress promoted oxygen enrichment of DOM secreted by roots to a small degree.

Examining plots of DBE versus carbon numbers for control (CK) versus 25 μmol L^{-1} Cd-treated samples (Fig. 5a) and control versus 200 μmol L^{-1} Cd-treated samples (Fig. 5b) suggests that most of the disappeared molecules had a higher carbon number than the produced molecules, which could indicate that Cd can catalytically degrade compounds with a high carbon number to produce compounds with lower carbon numbers, as also reported in *Rhus chinensis* plants grown in

Pb-contaminated soil (Zhu et al., 2019). The major subcategories of root exudate DOM in samples from all treatments were CHO, CHON, CHOS, and CHONS compounds, of varying proportions (Fig. 5c). CHO compounds accounted for the largest proportion in DOM in all samples. The relative proportions of CHON compounds decreased and CHOS and CHONS compounds increased in the 25 μmol L^{-1} Cd treatment, while CHON and CHONS compounds increased in the 200 μmol L^{-1} Cd treatment compared with the control. The weighted average N value increased with increasing Cd concentration, whilst the intensity-weighted average S value increased from 0.23 for CK to 0.29 for Cd-25, and then decreased to 0.22 (Table S3). These results suggest a dose response relationship in production/release of N-containing compounds in *E. annuus* under Cd stress, whilst for S-containing compounds there is increased production/release under low Cd stress conditions which then stabilized in the higher Cd treatment examined in our study. The major classes of DOM in samples from all three treatments were lignins/carboxylic rich alicyclic molecules (CRAM)-like structures, aliphatic/proteins and tannins, of which CRAM-like structures were the most abundant compound (Fig. 5d).

To further understand the molecular basis of detoxification mechanisms for Cd in roots of *E. annuus*, we assessed the molecular formulae and changes of DOM elemental compositions and biochemical classes between root exudate from the control and each of the 25 and 200 μmol L^{-1} Cd treatments. Unique CK formulae represent compounds that disappeared under Cd stress, whereas unique formulae identified in Cd-25/Cd-200 samples are newly produced molecules, and the common formulae represent DOM molecules that remained after exposure to Cd. The van Krevelen diagrams were divided into regions (Table S4) corresponding to six distinct biochemical classes of compounds identified in DOM of natural organic matter by Yuan et al. (2017). It is noted that this approach and the interpretations drawn from it are qualitative, since the compound classifications are generalizations, FT-ICR MS does not provide structural information that can help understand the biochemical processes and effects of the molecules identified, and also the FT-ICR MS
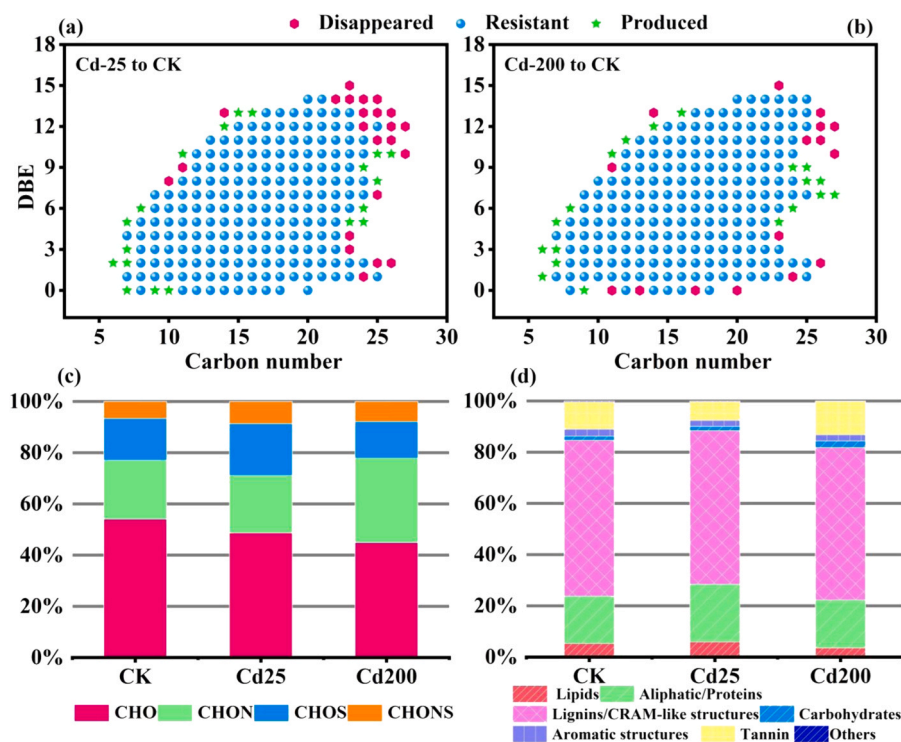
Fig. 5. (a) Double bond equivalent (DBE) versus carbon number in root exudate DOM of *E. annuus* grown for 15 d in the sample exposed to 25 compared to 0 μmol L^{-1} Cd, (b) DBE versus carbon number in root DOM of *E. annuus* grown for 15 d in the sample exposed to 200 compared to 0 μmol L^{-1} Cd. Bar charts show (c) the % relative contribution of the major subcategories and (d) major classes in the CK, Cd-25 and Cd-200 samples.

analyses were not conducted on replicate samples from the different Cd treatments. Nevertheless, our interpretations can help in suggesting tentative mechanisms that may be investigated in future, more-targeted experiments.

The van Krevelen diagram comparing the samples from the control and 25 µmol L^{-1} Cd treatment (Fig. 6a, c) showed that lignins/CRAM-like structures (label 3) were the most abundant and refractory compounds, followed by aliphatic/proteins (label 2) and lipids (label 1). Tannins (label 6), aromatic structures (label 5) and carbohydrates (label 4) were the most-susceptible DOM compounds to decomposition in the 25 µmol L^{-1} Cd stressed samples (Fig. 6c). The weighted average double bond equivalent (DBE) value decreased from 5.86 for CK to 4.84 for Cd-25 (Table S3), indicating degradation of compounds with aromatic structures to produce more aliphatic compounds under low Cd stress (Zhu et al., 2019). CRAM-structures comprise the majority of carbonyl-containing species with isolated, aliphatic ketones and several carboxyl groups. In contrast, lignin is a complex, high molecular weight biopolymer that contains reducible groups, and is composed of phenylpropanoids, primarily linked by ethers (Yuan et al., 2017). Aliphatic/proteins and lipids are compounds containing negatively charged organic groups, such as amino, thiol, hydroxyl and carboxyl groups (Kranthi et al., 2018). These groups can effectively bind heavy metal cations to form precipitates (Haynes, 1980), thus reducing Cd^{2+} entry into root cells of *E. annuus*. Grouping the DOM molecules based on their elemental composition (Fig. 6d), further demonstrated that low Cd stress promoted an increase in S-containing compounds.

Comparison of the molecular formulae and changes of DOM elemental compositions and biochemical classes between root exudate DOM from the control and 200 µmol L^{-1} Cd treatments (Fig. 6e-g), revealed that lignins/CRAM-like structures (label 3) were the most abundant and refractory compounds, followed by aliphatic/proteins (label 2), tannins (label 6) and lipids (label 1). Aromatic structures (label 5) and lipids (label 1) were the most-susceptible DOM compounds to decomposition in the 200 µmol L^{-1} Cd-exposed samples. Interestingly, higher proportions of aliphatic/proteins (label 2), carbohydrates (label 4), aromatic structures (label 5) and tannins (label 6) in root exudate DOM were newly produced in the 200 compared to the 25 µmol L^{-1} Cd

treatment. (Fig. 6g). Carbohydrates are polyhydroxy aldehydes or ketones whose hydroxyl functional groups interact with PTEs to gradually adsorb Cd^{2+} in solution (Kranthi et al., 2018). Aromatic structures contain a large number of carboxylic, carbonyl, hydroxyl, and ester groups, which play an important role in the adsorption of PTE ions (Zhao et al., 2019). In addition, tannins can be used as hydrogen donors to release hydrogen and combine with free radicals in the environment, preventing free radicals from causing oxidative damage to plants (Kraus et al., 2003). Based on this, we suggest that the production of carbohydrates, aromatic structures and tannins in DOM secreted by roots is an important Cd tolerance mechanism in *E. annuus*.

There are more disappeared than newly produced molecules in DOM from the 25 µmol L^{-1} Cd treatment compared to the control (Fig. 6b), whilst the opposite occurs for the 200 µmol L^{-1} Cd treatment compared to the control (Fig. 6f). The higher proportion of newly produced molecules in the Cd-200 treatment (10.6%) compared to the Cd-25 treatment (4.95%), indicates that root DOM of *E. annuus* has more active detoxification mechanisms under higher Cd stress.

4. Conclusions

This study indicated for the first time that DOM secreted by plant roots was involved in the resistance of plants to Cd-induced stress. This finding significantly increases our understanding of the mechanisms involved in metal tolerance and detoxification by plants. The stable existence of lignins/CRAM-like structures, aliphatic/proteins and lipids in DOM secreted by roots enhanced the ability of *E. annuus* to tolerate Cd stress. Carbohydrates, aromatic structures and tannins also played an important role in plant tolerance to high Cd stress. Whilst this study focused primarily on the composition of root exudate DOM, there are other known (e.g. precipitation of PTEs in plaques on root surfaces) and unknown tolerance and detoxification mechanisms of plants to Cd stress. Further research on the morphology and transport mechanism of Cd in plants, as well as the molecular mechanisms of its detoxification is essential. This study investigated one plant species, grown in solution rather than soil, and exposed to Cd for only 15 days. Further research should apply the same techniques to other PTEs and hyperaccumulators
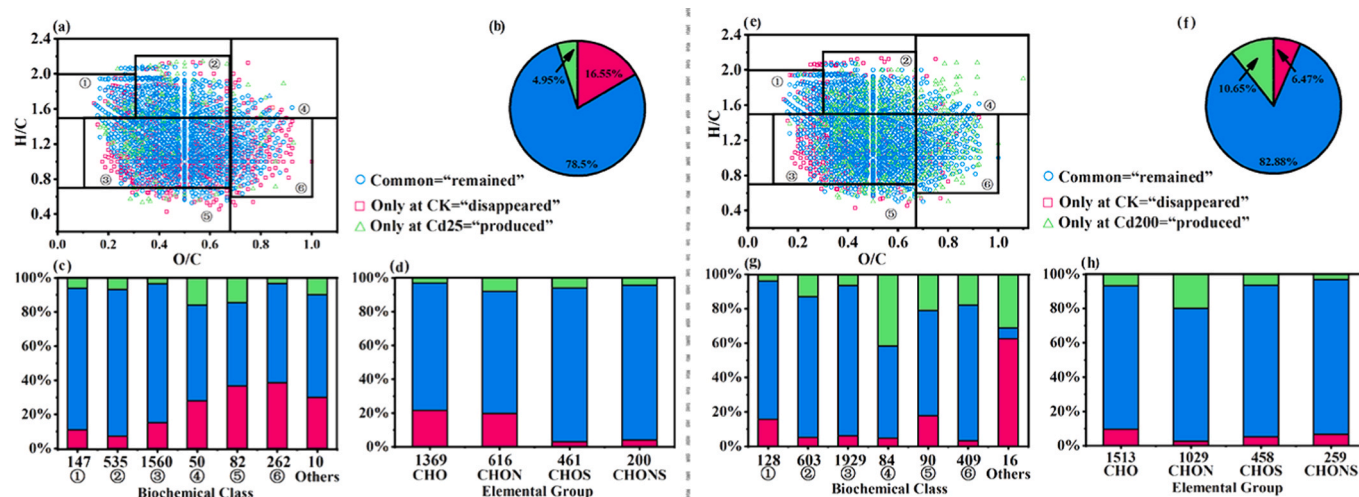
Fig. 6. Identification and comparison of molecules in root exudate DOM of *E. annuus* grown for 15 d in the sample exposed to 25/200 compared to 0 µmol L^{-1} Cd (CK – control). (a) van Krevelen diagram showing DOM formulae uniquely identified in CK (pink squares), formulae common to both CK and Cd-25 (blue circles), and formulae unique to Cd-25 (green triangles). Areas with numbers indicate different classes of identified DOM formulae: 1, lipids; 2, aliphatic/proteins; 3, lignins/carboxylic rich alicyclic molecules (CRAM)-like structures; 4, carbohydrates; 5, aromatic structures; and 6, tannins. (b) Percentages of DOM formulae identified only in CK (pink), common (blue) in CK and Cd-25, and only in Cd-25 (green). (c) and (g) Bar charts showing the percentages of identified DOM formulae by biochemical classes defined in panel (a)/(e). The number of DOM molecules in each biochemical class is shown on the x-axis. (d) and (h) Bar charts showing percentages of identified DOM formulae by elemental groups; the number of formulae identified in each group is shown on the x-axis. (e) van Krevelen diagram showing unique DOM formulae identified in CK (pink squares), formulae common to CK and Cd-200 (blue circles), and unique formulae in Cd-200 (green triangles). The numbers indicate different classes of identified DOM formulae as explained above. (f) Percentages of DOM formulae identified only in CK (pink), common (blue) in CK and Cd-200, and only in Cd-200 (green). (For interpretation of the references to color in this figure legend, the reader is referred to the web version of this article.)

grown in soil during longer field experiments.

Supporting information

Characterization of soil (S1). Plant culture conditions (S2). Measurement of plant leaf chlorophyll fluorescence parameters (S3). Details of analyses of plant material following harvesting (S4-S7). Plant growth characteristics (S8). Effect of Cd on plant ultrastructure (S9). Effect of Cd on membrane integrity (S10). Characterization of root exudate DOM (S11).

CRediT authorship contribution statement

Hong Zhang: Formal analysis, Investigation, Validation, Data Curation, Software, Writing-Original Draft; **Kate Heal**: Supervision, Writing - Review & Editing; **Xiangdong Zhu**: Investigation, Validation, Resources; **Mulualem Tigabu**: Writing - Review & Editing; **Yanan Xue**: Validation, Formal analysis, Data Curation; **Chuifan Zhou**: Conceptualization, Visualization, Resources, Supervision.

Declaration of Competing Interest

The authors declare that they have no known competing financial interests or personal relationships that could have appeared to influence the work reported in this paper.

Acknowledgments

Appendix A. Supporting information

Supplementary data associated with this article can be found in the online version at doi:10.1016/j.ecoenv.2021.112359.

References

Annu, Garg, A., Urmila, 2016. Level of Cd in different types of soil of Rohtak district and its bioremediation. J. Environ. Chem. Eng. 4, 3797–3802.

Bais, H.P., Weir, T.L., Perry, L.G., Gilroy, S., Vivanco, J.M., 2006. The role of root exudates in rhizosphere interactions with plants and other organisms. Annu. Rev. Plant Biol. 57, 233–266.

Bates, L.S., Waldren, R.P., Teare, I.D., 1973. Rapid determination of free proline for water-stress studies. Plant Soil 39, 205–207.

Chen, H.M., Yang, Z.M., Chu, R.K., Tolic, N., Liang, L.Y., Graham, D.E., Wullschleger, S. D., Gu, B., 2018. Molecular insights into Arctic soil organic matter degradation under warming. Environ. Sci. Technol. 52, 4555–4564.

Demmig, B., Winter, K., Krüger, A., Czygan, F., 1987. Photoinhibition and zeaxanthin formation in intact leaves: a possible role of the xanthophyll cycle in the dissipation of excess light energy. Plant Physiol. 84, 218–224.

Du, R., He, E., Tang, Y., Hu, P., 2011. How phytohormone IAA and chelator EDTA affect lead uptake by Zn/Cd hyperaccumulator *Picris divaricata*. Int. J. Phytoremediat. 13, 1024–1036.

Ekmekçi, Y., Tanyolaç, D., Ayhan, B., 2008. Effects of cadmium on antioxidant enzyme and photosynthetic activities in leaves of two maize cultivars. J. Plant Physiol. 165, 600–611.

Estrella-Gómez, N.E., Sauri-Duch, E., Zapata-Pérez, O., Santamaría, J.M., 2012. Glutathione plays a role in protecting leaves of *Salvinia minima* from Pb^{2+} damage associated with changes in the expression of SmGS genes and increased activity of GS. Environ. Exp. Bot. 75, 188–194.

Fu, X.P., Dou, C.M., Chen, Y.X., Chen, X.C., Shi, J.Y., Yu, M.G., Xu, J., 2011. Subcellular distribution and chemical forms of cadmium in *Phytolacca americana* L. J. Hazard. Mater. 186, 103–107.

Gill, S.S., Tuteja, N., 2010. Reactive oxygen species and antioxidant machinery in abiotic stress tolerance in crop plants. Plant Physiol. Biochem. 48, 909–930.

Gupta, D.K., Huang, H.G., Yang, X.E., Razafindrabe, B.H.N., Inouhe, M., 2010. The detoxification of lead in *Sedum alfredii* H. is not related to phytochelatins but the glutathione. J. Hazard. Mater. 177, 437–444.

Han, S.J., Li, X.N., Amombo, E., Fu, J.M., Xie, Y., 2018. Cadmium tolerance of perennial ryegrass induced by *Aspergillus aculeatus*. Front. Microbiol. 9, 1579. https://doi.org/10.3389/fmicb.2018.01579.

Hao, S.L., Zhu, X.D., Liu, Y.C., Qian, F., Fang, Z., Shi, Q., Zhang, S.C., Chen, J.M., Ren, Z. J., 2018. Production temperature effects on the structure of hydrochar-derived dissolved organic matter and associated toxicity. Environ. Sci. Technol. 52, 7486–7495.

Haynes, R.J., 1980. Ion exchange properties of roots and ionic interactions within the root apoplasm: their role in ion accumulation by plants. Bot. Rev. 46, 75–99.

Heraud, P., Beardall, J., 2000. Changes in chlorophyll fluorescence during exposure of *Dunaliella tertiolecta* to UV radiation indicate a dynamic interaction between damage and repair processes. Photosynth. Res. 63, 123–134.

Hissin, P.J., Hilf, R., 1976. A fluorometric method for determination of oxidized and reduced glutathione in tissues. Anal. Biochem. 74, 214–226.

Huang, M.Y., Zhu, H.H., Zhang, J., Tang, D.Y., Han, X.L., Chen, L., Du, D.Y., Yao, J., Chen, K., Sun, J., 2017. Toxic effects of cadmium on tall fescue and different responses of the photosynthetic activities in the photosystem electron donor and acceptor sides. Sci. Rep. 7, 14387.

Islam, E., Liu, D., Li, T.Q., Yang, X.E., Jin, X.F., Mahmood, Q., Tian, S.K., Li, J.Y., 2008. Effect of Pb toxicity on leaf growth, physiology and ultrastructure in the two ecotypes of *Elsholtzia argyi*. J. Hazard. Mater. 154, 914–926.

Kranthi, R.K., Kranthi, U.R., Bhargavi, E., Devi, I., Bhunia, B., 2018. Advances in exopolysaccharides based bioremediation of heavy metals in soil and water: a critical review. Carbohydr. Polym. 199, 353–364.

Kraus, T.E.C., Dahlgren, R.A., Zasoski, R.J., 2003. Tannins in nutrient dynamics of forest ecosystems - a review. Plant Soil 256, 41–66.

Li, X.M., Sun, G.X., Chen, S.C., Fang, Z., Yuan, H.Y., Shi, Q., Zhu, Y.G., 2018. Molecular chemodiversity of dissolved organic matter in paddy soils. Environ. Sci. Technol. 52, 963–971.

Lv, J.T., Zhang, S.Z., Wang, S.S., Luo, L., Cao, D., Christie, P., 2016. Molecular-scale investigation with ESI-FT-ICR-MS on fractionation of dissolved organic matter induced by adsorption on iron oxyhydroxides. Environ. Sci. Technol. 50, 2328–2336.

Monteiro, M.S., Santos, C., Soares, A.M.V.M., Mann, R.M., 2009. Assessment of biomarkers of cadmium stress in lettuce. Ecotoxicol. Environ. Saf. 72, 811–818.

Namdjoyan, S., Namdjoyan, S., Kermanian, H., 2012. Induction of phytochelatin and responses of antioxidants under cadmium stress in safflower (*Carthamus tinctorius*) seedlings. Turk. J. Bot. 36, 495–502.

Pinto, A.P., Simões, I., Mota, A.M., 2008. Cadmium impact on root exudates of sorghum and maize plants: a speciation study. J. Plant Nutr. 31, 1746–1755.

Rüegsegger, A., Schmutz, D., Brunold, C., 1990. Regulation of glutathione synthesis by cadmium in *Pisum sativum* L. Plant Physiol. 93, 1579–1584.

Seidel, M., Yager, P.L., Ward, N.D., Carpenter, E., Gomes, H.D.R., Krusche, A.V., Richey, J.E., Dittmar, T., Medeiros, P.M., 2015. Molecular-level changes of dissolved organic matter along the Amazon River-to-ocean continuum. Mar. Chem. 177, 218–231.

Sun, Y.B., Zhou, Q.X., Wang, L., Liu, W.T., 2009. Cadmium tolerance and accumulation characteristics of *Bidens pilosa* L. as a potential Cd-hyperaccumulator. J. Hazard. Mater. 161, 808–814.

Van Assche, F., Clijsters, H., 1990. Effects of metals on enzyme activity in plants. Plant Cell Environ. 13, 195–206.

Verkleij, J.A.C., Schat, H., Shaw, A.J., 1990. Mechanisms of metal tolerance in higher plants. Heavy Metal Tolerance in Plants Evolutionary Aspects, pp. 179–194.

Wagner, S., Riedel, T., Niggemann, J., Vähätalo, A.V., Dittmar, T., Jaffé, R., 2015. Linking the molecular signature of heteroatomic dissolved organic matter to watershed characteristics in world rivers. Environ. Sci. Technol. 49, 13798–13806.

Wang, X.L., Chang, Q.S., Hou, X.L., Lei, M., Ma, X.Q., 2010. Enrichment characteristics of heavy metals by plants in Sanming lead-zinc mining area. Ecol. Environ. Sci. 19, 108–112 (in Chinese).

Xie, Y.H., Huang, B.J., Ji, X.H., Tian, F.X., Wu, J.M., Guan, D., 2017. Evaluation of remediation effects of soil conditioners dedicated for Cd polluted paddy fields. Hunan Agric. Sci. 12, 31–35.

Yamamoto, Y., Kobayashi, Y., Matsumoto, H., 2001. Lipid peroxidation is an early symptom triggered by aluminum, but not the primary cause of elongation inhibition in pea roots. Plant Physiol. 125, 199–208.

Yang, S.L., Lan, S.S., Gong, M., 2009. Hydrogen peroxide-induced proline and metabolic pathway of its accumulation in maize seedlings. J. Plant Physiol. 166, 1694–1699.

Yuan, Z.W., He, C., Shi, Q., Xu, C.M., Li, Z.S., Wang, C.Z., Zhao, H.Z., Ni, J.R., 2017. Molecular insights into the transformation of dissolved organic matter in landfill leachate concentrate during biodegradation and coagulation processes using ESI FT-ICR MS. Environ. Sci. Technol. 51, 8110–8118.

Yuan, Y.H., Shu, S., Li, S.H., He, L.Z., Li, H., Du, N.S., Sun, J., Guo, S.R., 2014. Effects of exogenous putrescine on chlorophyll fluorescence imaging and heat dissipation capacity in cucumber (*Cucumis sativus* L.) under salt stress. J. Plant Growth Regul. 33, 798–808.

Zhao, C., Gao, S.J., Zhou, L., Li, X., Chen, X., Wang, C.C., 2019. Dissolved organic matter in urban forestland soil and its interactions with typical heavy metals: a case of Daxing District, Beijing. Environ. Sci. Pollut. Res. 26, 2960–2973.

Zhao, K., Wu, Y.Y., 2018. Effect of Zn deficiency and excessive bicarbonate on the allocation and exudation of organic acids in two Moraceae plants. Acta Geochim. 37, 125–133.

Zhao, L.J., Xie, J.F., Zhang, H., Wang, Z.T., Jiang, H.J., Gao, S.L., 2018. Enzymatic activity and chlorophyll fluorescence imaging of maize seedlings (*Zea mays* L.) after exposure to low doses of chlorsulfuron and cadmium. J. Integr. Agric. 17, 826–836.

Zhou, C.F., Huang, M.Y., Ren, H.J., Yu, J.D., Wu, J.M., Ma, X.Q., 2017. Bioaccumulation and detoxification mechanisms for lead uptake identified in *Rhus chinensis* Mill. seedlings. Ecotoxicol. Environ. Saf. 142, 59–68.

Zhou, C.F., Zhang, K., Lin, J.W., Li, Y., Chen, N.L., Zou, X.H., Hou, X.L., Ma, X.Q., 2015. Physiological responses and tolerance mechanisms to cadmium in *Conyza canadensis*. Int. J. Phytoremediat. 17, 280–289.

Zhu, X.D., Qian, F., Zhou, C.F., Li, L.J., Shi, Q., Zhang, S.C., Chen, J.M., 2019. Inherent metals of a phytoremediation plant influence its recyclability by hydrothermal liquefaction. Environ. Sci. Technol. 53, 6580–6586.